Geophysical Research Letters

Greening in Rural Areas Increases the Surface Urban Heat Island Intensity

Rui Yao[1], Lunche Wang[1] [iD], Xin Huang[2,3], Wei Gong[2], and Xiangao Xia[4]

[1]Hubei Key Laboratory of Critical Zone Evolution, School of Earth Sciences, China University of Geosciences, Wuhan, China, [2]State Key Laboratory of Information Engineering in Surveying, Mapping and Remote Sensing, Wuhan University, Wuhan, China, [3]School of Remote Sensing and Information Engineering, Wuhan University, Wuhan, China, [4]Key Laboratory of Middle Atmosphere and Global Environment Observation, Institute of Atmospheric Physics, Chinese Academy of Sciences, Beijing, China

Abstract In this study, Moderate Resolution Imaging Spectroradiometer land cover, land surface temperature (LST), and enhanced vegetation index (EVI) data were used to investigate the trends of surface urban heat island intensity (SUHII, urban LST minus rural LST) and their relations with vegetation in 397 global big cities during 2001–2017. Major findings include the following: (1) Annual daytime and nighttime SUHII increased significantly ($p < 0.05$, Mann-Kendall trend test) in 42.1% and 30.5% cities, respectively. (2) The daytime SUHII in the growing season was significantly and positively correlated with rural EVI in 58.9% cities. This is because high rural EVI can increase the EVI difference between urban and rural areas. (3) Rural greening contributed 22.5% of the increased daytime SUHII in the growing season at the global scale. This study highlights that the effect of greening in rural areas was a significant and widespread driver for the increased daytime SUHII.

Plain Language Summary Surface urban heat island (SUHI) refers to higher land surface temperature (LST) in urban than in rural areas. The increased SUHI intensity (urban LST minus rural) was mainly attributed to increased anthropogenic heat emission and built-up areas and reductions in vegetation in urban areas in the literature. However, this study showed that the increased vegetation (i.e., greening) in rural areas was a significant and widespread driver for the increased daytime SUHI intensity around the world during 2001–2017. The implication of this study is that urban LST may increase much faster than rural LST in future global warming.

1. Introduction

Urban heat island (UHI) effect refers to a higher land surface or air temperature in urban than in nearby rural areas. It can bring many adverse effects to human and environment (e.g., increasing mortality and energy consumption, and affecting water and air quality), thus receiving increasingly attention globally (Cao et al., 2018; Grimm et al., 2008; Luo & Lau, 2018; McCarthy et al., 2010).

Satellite remote sensing is one of the most widely used methods to study UHI. Land surface temperatures (LSTs) derived from satellite sensor can be used to estimate the surface UHI (SUHI) from the contrast between urban pixels and surrounding rural ones (Zhou et al., 2019). The spatial and temporal variations of SUHI have been documented, the SUHI intensity (SUHII, urban LST minus rural LST) differed greatly by cities, monitoring times and seasons according to previous studies (Clinton & Gong, 2013; Imhoff et al., 2010; Wang et al., 2015; Zhou et al., 2014). However, the long-term trends of SUHI at the global scale were only investigated by Chakraborty and Lee (2019), showing that the trends of annual daytime and nighttime SUHII during 2003–2017 were 0.03 °C per decade and 0.00 °C per decade, respectively. However, Chakraborty and Lee (2019) only computed the trends of annual mean SUHII and did not provide any seasonal differences. In addition, the data and methods in Chakraborty and Lee (2019) may lead to some uncertainties (for further discussion, see section 3.1). A systematic evaluation of SUHII and related drivers at a global scale is still needed.

One of the most important factors explaining observed SUHI is the reductions of vegetation in urban areas and the presences of vegetation outside cities, because vegetation can decrease the LST through transpiration during the daytime (Peng et al., 2012; Yao et al., 2017). Existing studies showed that the Earth is greening (Los, 2013; Zhang et al., 2017; Zhu et al., 2016). For example, Zhang et al. (2017) showed that global

vegetation (as reflected by enhanced vegetation index [EVI] and normalized difference vegetation index [NDVI]) showed a significant increasing trend from 2001 to 2015. Zeng et al. (2017) showed that greening of the Earth has slowed down the increase in global air temperature by 0.09 °C during 1982–2011. The increased evapotranspiration can explain 70% of this change. Liu et al. (2015) found that the trends of urban NDVI differed greatly by 50 global major cities, while the rural NDVI increased in most cities for the period 2001–2010. However, two questions still remain unclear: (1) What is the trend of SUHII change in major global cities in recent years? (2) Does the greening in rural areas affect the changes in SUHII?

This study aims at answering above two questions. Moderate Resolution Imaging Spectroradiometer (MODIS) LST and EVI data were utilized to analyze: (1) temporal trends of LST and SUHII in 397 global big cities, (2) the temporal relationships between SUHII and EVI across 2001–2017 in each city, and (3) the contribution of greening to the SUHII.

2. Materials and Methods

2.1. Extracting Urban and Rural Areas

In this study, land cover information was extracted from MODIS version 6 MCD12Q1 data (500-m spatial resolution, International Geosphere-Biosphere Programme classification layer, yearly composite, available from 2001 to 2016; Menashe & Friedl, 2018). Pixels classified as urban areas (digital number = 13) and water bodies (digital number = 17) in land cover maps (raster files) were converted into polygon (vector files) using the Environment for Visualizing Images 5.1 software (Menashe & Friedl, 2018). The land cover data in 2016 was used to analyze the trends of EVI and SUHII and their relationships during 2001–2017. The urban areas in 2016 can include old and new urban areas due to urbanization. Using urban areas in 2016 can reveal overall trends of EVI and SUHII and their relationships, including the information from old (without urbanization) and new urban areas (with urbanization) (Peng et al., 2018; Yao, Wang, Huang, Zhang, et al., 2018). Cities with urban area size larger than 200 km^2 were analyzed; thus, a total of 397 cities were investigated (Table S1). In addition, rural areas were defined as 10- to 30-km buffers around urban areas (removing water bodies, urban areas, and their 3-km buffer areas). The reasons for selecting 10- to 30-km buffers are as follows: (1) The extents of SUHI and urbanization are generally greater than urban area size (Zhang et al., 2004; Zhou et al., 2015); thus, the buffer zones were not set near the urban areas; and (2) to reduce uncertainties caused by different climate conditions, the buffer zones were not set farther (Luo & Lau, 2018; Yao, Wang, Huang, Niu, et al., 2018; Zhou et al., 2015). Meanwhile, other buffer radii were also used. Finally, altitude effects were not excluded from rural areas in this study since (1) it can influence the estimation of SUHII but it may not influence the estimation of the trends of SUHII and (2) it can retain more pixels and natural forests (mainly in high altitude areas) in rural areas and may reflect the changes in rural LST more accurately (Yao, Wang, Huang, Niu, et al., 2018).

2.2. Analyzing the Temporal Trends of LST and SUHII

Vegetation greenness information was derived from version 6 MOD13A3 EVI data (1-month composite, 1,000-m spatial resolution, 2001–2017). LST information was extracted from version 6 MOD11A2 data (8-day composite, 1,000-m spatial resolution, 2001–2017). These data have been widely validated and utilized (Eleftheriou et al., 2018; Huete et al., 2002; Li et al., 2018; Wan, 2008; Wang et al., 2015; Yao, Wang, Huang, Chen, et al., 2018). The LST was averaged into seasons and the growing season: in Northern Hemisphere (latitude higher than 0), the spring, summer, autumn, winter, and the growing seasons were defined as from March to May, June to August, September to November, December to February, and April to October, respectively. In Southern Hemisphere (latitude lower than 0), the spring, summer, autumn, winter, and the growing seasons were defined as from September to November, December to February, March to May, June to August, and October to April, respectively. We only analyzed the EVI in the growing season, since in late autumn, winter, and early spring, the vegetation activity is low and the EVI may be affected by snow and ice in cold regions (Huete et al., 2002; Piao, 2003).

The SUHII was computed utilizing equation (1) (Peng et al., 2012; Zhou et al., 2014):

$$\Delta LST = LST_{urban} - LST_{rural}, \tag{1}$$

where the LST_{urban}, LST_{rural}, and ΔLST represent the urban LST, rural LST, and SUHII, respectively. ΔEVI were computed using the same method as equation (1). The temporal trends of LST and SUHII for the period 2001–2017 were analyzed using the Mann-Kendall test and Sen's slope (Kendall, 1975; Mann, 1945; Sen, 1968). Mann-Kendall test is considered as a robust method for detecting trends and was highly recommended by World Meteorological Organization (1988; Shadmani et al., 2012).

2.3. The Effects of the Change in Rural EVI on SUHII

Spearman's correlation analyses and Spearman's correlation analyses after detrending were employed to investigate the temporal relationships between SUHII and EVI or ΔEVI in the growing season in each city across 2001–2017. The effects of the change in rural EVI on rural LST in the growing season over the period 2001–2017 were calculated using equation (2):

$$E_{EVI} = Trend\ (LST_{rural} - LST_{rer}) \tag{2}$$

where the LST_{rural} represents the LST in rural areas. LST_{ref} is the reference LST. E_{EVI} is the effects of the change in rural EVI on rural LST. We calculated the LST_{ref} using following steps. First, in each pixel of the globe, the slope (Mann-Kendall test and Sen's slope) of the growing season EVI during 2001–2017 was calculated. Second, in the LST maps, pixels with absolute value of slope of the growing season EVI higher than 10th percentile (other thresholds were also used) of the slopes in all global pixels (equal to 0.000114 in this study) were excluded. Finally, the LST_{ref} of each city in each year was calculated as the average LST of valid (not excluded in the second step) pixels in rural areas. After that, E_{EVI} was computed as the trend of difference between LST_{rural} and LST_{ref}. This is based on the hypothesis that if rural EVI does not change, the LST_{rural} will be the same as LST_{ref}. This hypothesis is similar to the methods in which we calculated the trends of SUHII. In addition, the opposite number of E_{EVI} can be regarded as the effects of the change in rural EVI on SUHII.

3. Results and Discussion

3.1. Temporal Trends of SUHII

Annual average daytime and nighttime SUHII increased (slope > 0) significantly ($p < 0.05$) in 42.1% and 30.5% cities, respectively (Figure 1). Few cities showed significant decreasing trends of SUHII. Seasons with maximum and minimum numbers of cities with significant increasing trends of daytime SUHII were summer (38.3% cities) and winter (17.1% cities), respectively. Comparatively, the trends of nighttime SUHII differed little by seasons.

On average, annual daytime and nighttime SUHII increased at the rate of 0.29 ± 0.41 °C per decade (mean and standard deviation, hereafter) and 0.10 ± 0.23 °C per decade, respectively (Table 1). The trends of daytime and nighttime SUHII in the growing season averaged for 397 cities were 0.41 ± 0.49 and 0.13 ± 0.24 °C per decade, respectively. These trends were close to the trends in summer. This is understandable, since the growing season defined in this study (from April to October) includes the whole summer (from June to August). Furthermore, the standard deviations of the trends of daytime SUHII across cities were larger than that of trends of nighttime SUHII. This indicated that the trends of nighttime SUHII were more consistent across cities. The large difference in the trends of daytime SUHII across cities may be attributed to large difference in daytime SUHII across cities. The daytime SUHII differed greatly by cities, ranging from negative SUHII in cities surrounded by deserts to over 7 °C in cities surrounded by forest. However, nighttime SUHII differed slightly by cities (Imhoff et al., 2010; Peng et al., 2012). One of the major reasons is that vegetation transpiration can decrease the LST during the daytime rather than nighttime (Imhoff et al., 2010; Peng et al., 2012). Thus, the transformation of natural land surface to built-up areas over time may lead to a higher increasing rate of daytime SUHII in cities with higher daytime SUHII but a stable trend in cities with insignificant daytime SUHII. In addition, the great difference in the trends of daytime SUHII across seasons mentioned above may be attributed to similar reasons.

Chakraborty and Lee (2019) found that the global average trends of annual daytime and nighttime SUHII during 2003–2017 were 0.03 and 0.00 °C per decade, respectively. The rates were much lower than the
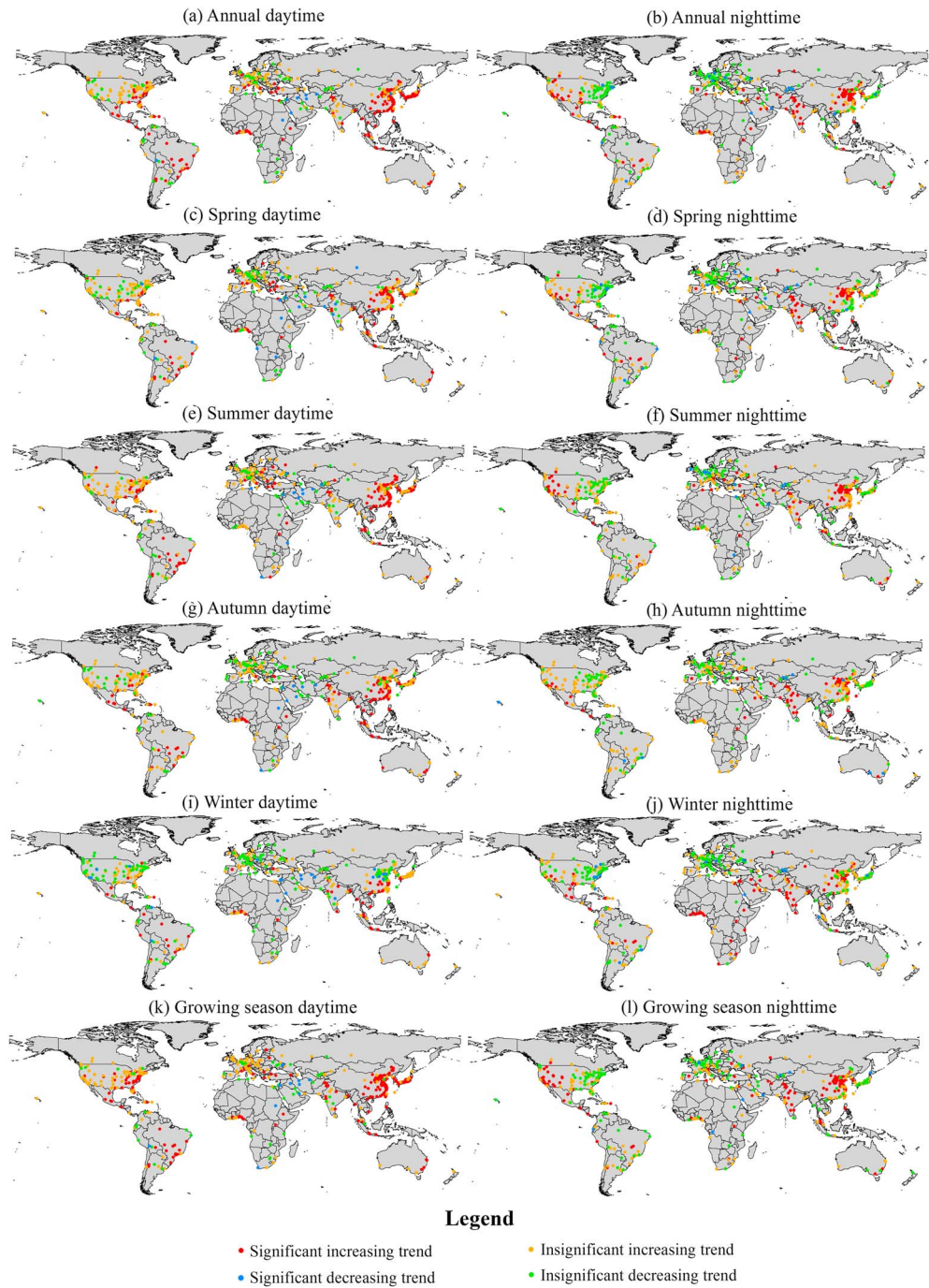
AGU
100
ADVANCING EARTH
AND SPACE SCIENCE

Geophysical Research Letters

10.1029/2018GL081816

(a) Annual daytime

(b) Annual nighttime

(c) Spring daytime

(d) Spring nighttime

(e) Summer daytime

(f) Summer nighttime

(g) Autumn daytime

(h) Autumn nighttime

(i) Winter daytime

(j) Winter nighttime

(k) Growing season daytime

(l) Growing season nighttime

Legend

• Significant increasing trend   • Insignificant increasing trend

• Significant decreasing trend   • Insignificant decreasing trend

Figure 1. Trends of surface urban heat island intensity in annual, each season and growing season.

present study (Table 1). Chakraborty and Lee (2019) used urban area map in 2001 and calculated the SUHII as the difference in LST between urban and neighboring suburban areas. The trends of SUHII may be underestimated by Chakraborty and Lee (2019) since (1) the SUHI's spatial extent is greater than the actual urban area size (Yao, Wang, Huang, Niu, et al., 2018; Zhang et al., 2004; Zhou et al., 2015) and (2) urbanization generally happened in suburban areas (Yao, Wang, Huang, Niu, et al., 2018; Yao et al., 2017; Zhou et al., 2016).

Spatially, the temporal trends of SUHII differed by cities (Figure 1). First, the daytime SUHII increased significantly in most Chinese cities except in winter. This is similar to previous studies and primarily due to the

Table 1
Temporal Trends (Mean and Standard Deviation) of EVI, ΔEVI, LST, and SUHII Averaged for 397 Cities

	EVI in urban (per decade)	EVI in rural (per decade)	ΔEVI (per decade)
	-0.0045 ± 0.0167	0.0121 ± 0.0149	-0.0163 ± 0.0197
Growing season	LST in urban (°C per decade)	LST in rural (°C per decade)	SUHII (°C per decade)
Annual daytime	0.46 ± 0.54	0.18 ± 0.48	0.29 ± 0.41
Annual nighttime	0.47 ± 0.31	0.37 ± 0.25	0.10 ± 0.23
Spring daytime	0.53 ± 0.74	0.19 ± 0.70	0.33 ± 0.53
Spring nighttime	0.46 ± 0.42	0.38 ± 0.36	0.10 ± 0.31
Summer daytime	0.60 ± 0.77	0.16 ± 0.64	0.45 ± 0.56
Summer nighttime	0.54 ± 0.50	0.40 ± 0.36	0.12 ± 0.29
Autumn daytime	0.41 ± 0.67	0.15 ± 0.59	0.28 ± 0.44
Autumn nighttime	0.49 ± 0.47	0.39 ± 0.38	0.10 ± 0.24
Winter daytime	0.35 ± 0.73	0.30 ± 0.79	0.08 ± 0.48
Winter nighttime	0.42 ± 0.56	0.35 ± 0.59	0.09 ± 0.34
Growing season daytime	0.61 ± 0.58	0.22 ± 0.49	0.41 ± 0.49
Growing season nighttime	0.59 ± 0.34	0.45 ± 0.25	0.13 ± 0.24

Note. EVI = enhanced vegetation index; LST = land surface temperature; SUHII = surface urban heat island intensity.

rapid urbanization in China (Luo & Lau, 2017; Yang et al., 2019; Yao et al., 2017). Second, cities with significant increasing trends of daytime SUHII in winter were generally located near the equatorial region (Figure 1i), which can be explained by the different vegetation species between this region (mainly covered by evergreen forest) and others (mainly covered by deciduous forest, seasonal crop, and grass; Yao et al., 2017). Evergreen forest is green and will be affected by driving factors (e.g., human activity and climate variability) in winter, while tree species in other regions are brown and may not be affected by driving forces in winter. Thus, the interannual variations in evergreen forest rather than other vegetation types will drive the SUHII in winter. This claim was demonstrated by Yao et al. (2017). Third, it seems that nighttime SUHII increased in most cities in relatively arid regions (Western United States and Northern China), while it was not true for cities in relatively humid regions (Eastern United States, Western Europe, and Southern China). This is similar to Chakraborty and Lee (2019) and may be attributed to the soil moisture effect (Peng et al., 2018; Yao et al., 2017; Zhou et al., 2014). The changes in soil moisture can affect thermal admittance and the changing rate of LST (Oke et al., 1991). Relatively arid regions generally have higher nighttime SUHII than relatively humid regions, since in relatively arid region the soil is dry and the rural LST decreases rapidly at night. Drier soil (in relatively arid regions) transformed into built-up areas with urbanization may result in higher slopes of nighttime SUHII than wetter soil (in relatively humid regions; Peng et al., 2018; Yao et al., 2017; Zhou et al., 2014).

3.2. Relationships Between SUHII and EVI or ΔEVI

Spearman's correlation analyses (without detrending) revealed that the daytime SUHII was significantly ($p < 0.05$) and positively ($r > 0$) linked to rural EVI in the growing season in 58.9% of the cities across 2001–2017 (Table 2). The results of Spearman's correlation analyses after detrending were similar to the results of above Spearman's correlation analyses. This suggested that the years with higher rural EVI were generally accompanied by higher daytime SUHII in the growing season in most cities. Meanwhile, increased rural EVI was one of the reasons for the increased daytime SUHII in the growing season, because high rural EVI can increase the EVI difference between urban and rural areas then increase the SUHII. The results showed that (1) the rural EVI was significantly and negatively correlated (Spearman's correlation without detrending) with the ΔEVI in 78.8% cities and (2) the ΔEVI was significantly and negatively related to SUHII over 62.7% cities (Table 2). Then high EVI difference between urban and rural areas can increase the SUHII (Peng et al., 2012; Yao et al., 2017). Comparatively, significant correlations between nighttime SUHII and rural EVI were observed in the minority of the cities (Table 2). Thus, high rural EVI may not increase the nighttime SUHII. This can be attributed to low transpiration of vegetation during the nighttime (Peng et al., 2012).

Table 2
Spearman's Correlations Analyses Without Detrending and After Detrending Between SUHII and EVI or ΔEVI

Without detrending	SUHII & rural EVI	SUHII & urban EVI	SUHII & ΔEVI
Growing season daytime	361(234), 36(5)	234(82), 163(57)	30(2), 367(249)
Growing season nighttime	206(64), 191(25)	101(13), 296(88)	127(11), 270(97)
After detrending			
Growing season daytime	331(155), 66(7)	263(94), 134(20)	48(2), 349(156)
Growing season nighttime	155(12), 242(35)	116(13), 281(51)	179(17), 218(25)

Note. The numbers of the cities with positive and negative Spearman's correlations are displayed at left and right, respectively. The numbers in brackets are the numbers of the cities with significant ($p < 0.05$) Spearman's correlations. EVI = enhanced vegetation index; SUHII = surface urban heat island intensity.

Significant Spearman's correlations between urban EVI and daytime SUHII in the growing season were only found in the minority of the cities (Table 2), indicating that urban EVI may have fewer influences on daytime SUHII in the growing season (detailed explanation in next paragraph). Negative correlations between nighttime SUHII and urban EVI in the growing season were observed in 74.6% cities. With urbanization, vegetation is replaced by built-up areas, which generally have higher nighttime LST than other land cover types. The increased built-up areas can increase the nighttime SUHII. Moreover, vegetation can pose a shading effect. It can decrease the heat stored in urban roads during the daytime, thus reducing the SUHII during the nighttime (Quan et al., 2016; Yao et al., 2017). These may be the primary reasons for negative correlations between nighttime SUHII and urban EVI.

It is worth noting that the number of cities with significant Spearman's correlations between daytime SUHII and rural EVI was much higher than that between daytime SUHII and urban EVI in the growing season across 2001–2017 (Table 2). The amount of vegetation in rural areas is generally higher than urban areas due to urbanization (except for certain cities in arid region). Therefore, more vegetation will be influenced by human activity and climate variability in rural than in urban areas. For example, the impact of drought on vegetation in rural areas with dense vegetation coverage may be larger than in urban areas with sparse vegetation coverage. Meanwhile, urbanization in developing cities (e.g., certain Asian and African cities) generally decreases the EVI and can offset the greening trend in urban areas (primarily due to planting and CO_2 fertilization; Figure S1b in the supporting information). The variations in EVI across years may be larger in rural than in urban areas (Yao, Wang, Huang, Chen, et al., 2018). We calculated the standard deviations of EVI in each city across 2001–2017 and the difference in the EVI standard deviations between urban and rural areas. The standard deviation of EVI was higher in rural than in urban areas in 82.9% cities. This was similar to Yao, Wang, Huang, Chen, et al. (2018), who reported that the Δstandard deviation of EVI (urban core minus rural) was negative in all of the 31 major Chinese cities in summer. The larger variations in rural EVI than urban EVI across 2001–2017 led to the dominant control of rural EVI on ΔEVI: (1) As mentioned above, the rural EVI was significantly and negatively related to ΔEVI in 78.8% cities. (2) The urban EVI was significantly and positively linked to ΔEVI in only 25.2% cities. The dominant control of rural EVI on ΔEVI was one of the reasons for the stronger correlation between SUHII and rural EVI than urban EVI.

3.3. The Effects of the Change in Rural EVI on SUHII

For 397 cities combined, the E_{EVI} were −0.09 and −0.03 °C per decade in the growing season during the daytime and nighttime, respectively. Therefore, if the rural EVI is stable, the slope of rural LST will be 0.09 °C per decade higher, and the slope of daytime SUHII will be 0.09 °C per decade lower in the growing season. The slope of daytime SUHII averaged for 397 cities is 0.41 °C per decade in the growing season (Table 1). Thus, the contribution of rural greening to the increased daytime SUHII in the growing season was 22.5%. In addition, the sensitivities of the experimental results to different thresholds (when analyzing the effects of the change in rural EVI on SUHII) and buffer radii (when selecting rural areas) were tested. For example, the contributions were 19.3% and 30.0% when using 15th and 5th percentiles as thresholds, respectively (using 10- to 30-km buffer as rural areas). The differences in contribution caused by different selection of rural areas were also relatively small (using 10th percentile as threshold, 10- to 40-km buffer: The contribution was 23.7%; 20- to 40-km buffer: The contribution was 24.1%). Furthermore, other factors (e.g., urbanization, soil moisture, and climate) contributed to the remaining part, which should be examined in future

research. Additionally, 186 cities showed significant increasing trends of daytime SUHII in the growing season. Among them, 44.6% (83) cities exhibited significant decreasing trends of E_{EVI}. This suggested that rural greening was not only a significant reason but also a widespread one for the increased daytime SUHII in the growing season. Spatially, most cities exhibited significant decreasing trends of E_{EVI} in China (Figure S2). This phenomenon may mostly be owing to the prominent greening trend in China (Figure S1).

The increased SUHII was mainly attributed to increased anthropogenic heat emission and built-up areas and reductions in vegetation in urban areas in the literature (Benas et al., 2016; Voogt & Oke, 2003; Weng, 2009; Yao et al., 2017, Yao, Wang, Huang, Zhang, et al., 2018; Zhou et al., 2016). The effect of greening in rural areas has not been documented in the literature but was an important and widespread driver for the increase in daytime SUHII according to the present study. Thus, some previous studies need to reevaluate the role of rural greening. Moreover, rural greening should arouse more attention in future SUHI's research.

3.4. Implications

The emission of greenhouse gas (e.g., CO_2 and CH_4) into the atmosphere by human activity leads to global warming. Recent studies suggested that the increase of CO_2 in the atmosphere may green the Earth and then slow the global warming (Los, 2013; Zeng et al., 2017; Zhu et al., 2016). However, the slopes of urban and rural EVI averaged for 397 cities were -0.0045 ± 0.0167 per decade and 0.0121 ± 0.0149 per decade, respectively (Table 1). Thus, vegetation greening may cool the daytime LST in rural areas rather than in urban areas and then increase the daytime SUHII. The implication was that urban LST increased much faster than the rural LST (Table 1). Meanwhile, the season with the highest increasing rate of daytime SUHII was summer (Table 1). This is probably because vegetation activity is the highest in summer. Therefore, if the global warming trends continued, the daytime SUHI effect may become more serious, especially in summer.

4. Conclusions

In the present study, MODIS LST and EVI data were utilized to analyze the trends of EVI and SUHII and their relationships at the global scale for the period 2001–2017. The results showed the following: (1) Annual average daytime and nighttime SUHII increased significantly in 42.1% and 30.5% cities, respectively. The trends of daytime SUHII differed greatly by cities and seasons, while it was not the case for the trends of nighttime SUHII. The season with the highest increasing rate of daytime SUHII was summer. (2) The daytime SUHII in the growing season was significantly and positively related to rural EVI in 58.9% cities. This is because high rural EVI can increase the EVI difference between urban and rural areas. (3) At the global scale, the contribution of rural greening to the increased daytime SUHII was 0.09 °C per decade (22.5%) in the growing season.

The effect of greening in rural areas was an important and widespread driver for the increase in daytime SUHII. Therefore, rural greening should arouse more attention in future. However, there are certain uncertainties in the present study. First, the study period (17 years) is a little short since MODIS data are available since 2000, which may be a major reason for the insignificant trends of SUHII and EVI in the majority of the global cities. Second, other factors (e.g., increased anthropogenic heat emission and built-up areas, reductions in vegetation in urban areas, and climate variability) contributing to most parts of the increase in SUHII were not investigated in this study. Third, the 1-km spatial resolution data are a little coarse for city-scale studies. Thus, future studies should (1) quantify the contributions of other factors (e.g., urbanization, soil moisture, and climate) to the increased SUHII of the globe and (2) systematically analyze the effect of rural greening on SUHII at regional and local scales using higher spatial resolution data for longer time series.

References

Benas, N., Chrysoulakis, N., & Cartalis, C. (2016). Trends of urban surface temperature and heat island characteristics in the Mediterranean. *Theoretical and Applied Climatology*, *130*, 807–816.

Cao, Q., Yu, D., Georgescu, M., Wu, J., & Wang, W. (2018). Impacts of future urban expansion on summer climate and heat-related human health in eastern China. *Environment International*, *112*, 134–146. https://doi.org/10.1016/j.envint.2017.12.027

Chakraborty, T., & Lee, X. (2019). A simplified urban-extent algorithm to characterize surface urban heat islands on a global scale and examine vegetation control on their spatiotemporal variability. *International Journal of Applied Earth Observation*, *74*, 269–280. https://doi.org/10.1016/j.jag.2018.09.015

Clinton, N., & Gong, P. (2013). MODIS detected surface urban heat islands and sinks: Global locations and controls. *Remote Sensing of Environment*, *134*, 294–304. https://doi.org/10.1016/j.rse.2013.03.008

Eleftheriou, D., Kiachidis, K., Kalmintzis, G., Kalea, A., Bantasis, C., Koumadoraki, P., et al. (2018). Determination of annual and seasonal daytime and nighttime trends of MODIS LST over Greece—Climate change implications. *Science of the Total Environment*, *616–617*, 937–947.

Grimm, N. B., Faeth, S. H., Golubiewski, N. E., Redman, C. L., Wu, J., Bai, X., & Briggs, J. M. (2008). Global change and the ecology of cities. *Science*, *319*(5864), 756–760. https://doi.org/10.1126/science.1150195

Huete, A., Didan, K., Miura, T., Rodriguez, E. P., X, G., & Ferreira, L. G. (2002). Overview of the radiometric and biophysical performance of the MODIS vegetation indices. *Remote Sensing of Environment*, *83*(1-2), 195–213. https://doi.org/10.1016/S0034-4257(02)00096-2

Imhoff, M. L., Zhang, P., Wolfe, R. E., & Bounoua, L. (2010). Remote sensing of the urban heat island effect across biomes in the continental USA. *Remote Sensing of Environment*, *114*(3), 504–513. https://doi.org/10.1016/j.rse.2009.10.008

Kendall, M. G. (1975). *Rank Correlation Methods*. London: Griffin.

Li, H., Zhou, Y., Li, X., Meng, L., Wang, X., Wu, S., & Sodoudi, S. (2018). A new method to quantify surface urban heat island intensity. *Science of the Total Environment*, *624*, 262–272. https://doi.org/10.1016/j.scitotenv.2017.11.360

Liu, Y., Wang, Y., Peng, J., Du, Y., Liu, X., Li, S., & Zhang, D. (2015). Correlations between urbanization and vegetation degradation across the world's metropolises using DMSP/OLS nighttime light data. *Remote Sensing*, *7*(2), 2067–2088. https://doi.org/10.3390/rs70202067

Los, S. O. (2013). Analysis of trends in fused AVHRR and MODIS NDVI data for 1982–2006: Indication for a CO_2 fertilization effect in global vegetation. *Global Biogeochemical Cycles*, *27*, 318–330. https://doi.org/10.1002/gbc.20027

Luo, M., & Lau, N. C. (2017). Heat waves in southern China: Synoptic behavior, long-term change, and urbanization effects. *Journal of Climate*, *30*(2), 703–720. https://doi.org/10.1175/JCLI-D-16-0269.1

Luo, M., & Lau, N. C. (2018). Increasing heat stress in urban areas of eastern China: Acceleration by urbanization. *Geophysical Research Letters*, *45*, 13,060–13,069. https://doi.org/10.1029/2018GL080306

Mann, H. B. (1945). Nonparametric tests against trend. *Econometrica*, *13*(3), 245–259. https://doi.org/10.2307/1907187

McCarthy, M. P., Best, M. J., & Betts, R. A. (2010). Climate change in cities due to global warming and urban effects. *Geophysical Research Letters*, *37*, L09705. https://doi.org/10.1029/2010GL042845

Menashe, D. S., & Friedl, M. A. (2018). User guide to collection 6 MODIS land cover (MCD12Q1 and MCD12C1) product. Retrieved from https://lpdaac.usgs.gov/sites/default/files/public/product_documentation/mcd12_user_guide_v6.pdf (accessed 20.05.2018)

Oke, T. R., Johnson, G. T., Steyn, D. G., & Watson, I. D. (1991). Simulation of surface urban heat islands under 'ideal' conditions at night. Part 2: Diagnosis of causation. Boundary-layer meteorology. *Boundary-Layer Meteorology*, *56*(4), 339–358. https://doi.org/10.1007/BF00119211

Peng, J., Ma, J., Liu, Q., Liu, Y., Hu, Y., Li, Y., & Yue, Y. (2018). Spatial-temporal change of land surface temperature across 285 cities in China: An urban-rural contrast perspective. *Science of the Total Environment*, *635*, 487–497. https://doi.org/10.1016/j.scitotenv.2018.04.105

Peng, S., Piao, S., Ciais, P., Friedlingstein, P., Ottle, C., Breon, F. M., et al. (2012). Surface urban heat island across 419 global big cities. *Environmental Science & Technology*, *46*(2), 696–703. https://doi.org/10.1021/es2030438

Piao, S. (2003). Interannual variations of monthly and seasonal normalized difference vegetation index (NDVI) in China from 1982 to 1999. *Journal of Geophysical Research*, *108*(D14), 4401. https://doi.org/10.1029/2002JD002848

Quan, J., Zhan, W., Chen, Y., Wang, M., & Wang, J. (2016). Time series decomposition of remotely sensed land surface temperature and investigation of trends and seasonal variations in surface urban heat islands. *Journal of Geophysical Research: Atmospheres*, *121*, 2638–2657. https://doi.org/10.1002/2015JD024354

Sen, P. K. (1968). Estimates of the regression coefficient based on Kendall's tau. *Journal of the American Statistical Association*, *63*(324), 1379–1389. https://doi.org/10.1080/01621459.1968.10480934

Shadmani, M., Marofi, S., & Roknian, M. (2012). Trend analysis in reference evapotranspiration using Mann-Kendall and Spearman's rho tests in arid regions of Iran. *Water Resources Management*, *26*(1), 211–224. https://doi.org/10.1007/s11269-011-9913-z

Voogt, J. A., & Oke, T. R. (2003). Thermal remote sensing of urban climates. *Remote Sensing of Environment*, *86*(3), 370–384. https://doi.org/10.1016/S0034-4257(03)00079-8

Wan, Z. (2008). New refinements and validation of the MODIS land-surface temperature/emissivity products. *Remote Sensing of Environment*, *112*(1), 59–74. https://doi.org/10.1016/j.rse.2006.06.026

Wang, J., Huang, B., Fu, D., & Atkinson, P. (2015). Spatiotemporal variation in surface urban heat island intensity and associated determinants across major Chinese cities. *Remote Sensing*, *7*(4), 3670–3689. https://doi.org/10.3390/rs70403670

Weng, Q. (2009). Thermal infrared remote sensing for urban climate and environmental studies: Methods, applications, and trends. *ISPRS Journal of Photogrammetry*, *64*(4), 335–344. https://doi.org/10.1016/j.isprsjprs.2009.03.007

World Meteorological Organization (1988). Analysing long time series of hydrological data with respect to climate variability. Wcap-3, WMO/TD-No. 224.

Yang, Q., Huang, X., & Tang, Q. (2019). The footprint of urban heat island effect in 302 Chinese cities: Temporal trends and associated factors. *Science of the Total Environment*, *655*, 652–662. https://doi.org/10.1016/j.scitotenv.2018.11.171

Yao, R., Wang, L., Huang, X., Chen, J., Li, J., & Niu, Z. (2018). Less sensitive of urban surface to climate variability than rural in northern China. *Science of the Total Environment*, *628–629*, 650–660.

Yao, R., Wang, L., Huang, X., Niu, Y., Chen, Y., & Niu, Z. (2018). The influence of different data and method on estimating the surface urban heat island intensity. *Ecological Indicators*, *89*, 45–55. https://doi.org/10.1016/j.ecolind.2018.01.044

Yao, R., Wang, L., Huang, X., Niu, Z., Liu, F., & Wang, Q. (2017). Temporal trends of surface urban heat islands and associated determinants in major Chinese cities. *Science of the Total Environment*, *609*, 742–754. https://doi.org/10.1016/j.scitotenv.2017.07.217

Yao, R., Wang, L., Huang, X., Zhang, W., Li, J., & Niu, Z. (2018). Interannual variations in surface urban heat island intensity and associated drivers in China. *Journal of Environmental Management*, *222*, 86–94. https://doi.org/10.1016/j.jenvman.2018.05.024

Zeng, Z., Piao, S., Li, L. Z. X., Zhou, L., Ciais, P., Wang, T., et al. (2017). Climate mitigation from vegetation biophysical feedbacks during the past three decades. *Nature Climate Change*, *7*(6), 432–436. https://doi.org/10.1038/nclimate3299

Zhang, X., Friedl, M. A., Schaaf, C. B., Strahler, A. H., & Schneider, A. (2004). The footprint of urban climates on vegetation phenology. *Geophysical Research Letters*, *31*, L12209. https://doi.org/10.1029/2004GL020137

Zhang, Y., Song, C., Band, L. E., Sun, G., & Li, J. (2017). Reanalysis of global terrestrial vegetation trends from MODIS products: Browning or greening? *Remote Sensing of Environment*, *191*, 145–155. https://doi.org/10.1016/j.rse.2016.12.018

Zhou, D., Xiao, J., Bonafoni, S., Berger, C., Deilami, K., Zhou, Y., et al. (2019). Satellite remote sensing of surface urban heat islands: Progress, challenges, and perspectives. *Remote Sensing*, *11*, 48.

Zhou, D., Zhang, L., Hao, L., Sun, G., Liu, Y., & Zhu, C. (2016). Spatiotemporal trends of urban heat island effect along the urban development intensity gradient in China. *Science of the Total Environment*, *544*, 617–626. https://doi.org/10.1016/j.scitotenv.2015.11.168

Zhou, D., Zhao, S., Liu, S., Zhang, L., & Zhu, C. (2014). Surface urban heat island in China's 32 major cities: Spatial patterns and drivers. *Remote Sensing of Environment*, *152*, 51–61. https://doi.org/10.1016/j.rse.2014.05.017

Zhou, D., Zhao, S., Zhang, L., Sun, G., & Liu, Y. (2015). The footprint of urban heat island effect in China. *Scientific Reports*, *5*(1), 11160. https://doi.org/10.1038/srep11160

Zhu, Z., Piao, S., Myneni, R. B., Huang, M., Zeng, Z., Canadell, J. G., et al. (2016). Greening of the Earth and its drivers. *Nature Climate Change*, *6*(8), 791–795. https://doi.org/10.1038/nclimate3004